Published in final edited form as:
J Geophys Res. 2008 January 1; 113: . doi:10.1029/2007JB005035.

One-, two- and three-phase viscosity treatments for basaltic lava flows

Andrew J. L. Harris[1] and **John S. Allen III**[2]

[1]HIGP/SOEST, University of Hawai'i, 1680 East-West Road, Honolulu, HI 96822, USA. (harris@higp.hawaii.edu)

[2]Department of Mechanical Engineering, University of Hawai'i, 1680 East-West Road, Honolulu, HI 96822, USA

Abstract

Lava flows comprise three-phase mixtures of melt, crystals, and bubbles. While existing one-phase treatments allow melt phase viscosity to be assessed on the basis of composition, water content, and/or temperature, two-phase treatments constrain the effects of crystallinity or vesicularity on mixture viscosity. However, three-phase treatments, allowing for the effects of coexisting crystallinity and vesicularity, are not well understood. We investigate existing one- and two-phase treatments using lava flow case studies from Mauna Loa (Hawaii) and Mount Etna (Italy) and compare these with a three-phase treatment that has not been applied previously to basaltic mixtures. At Etna, melt viscosities of 425 ± 30 Pa s are expected for well-degassed (0.1 w. % H_2O), and 135 ± 10 Pa s for less well-degassed (0.4 wt % H_2O), melt at 1080°C. Application of a three-phase model yields mixture viscosities (45% crystals, 25–35% vesicles) in the range 5600–12,500 Pa s. This compares with a measured value for Etnean lava of 9400 ± 1500 Pa s. At Mauna Loa, the three-phase treatment provides a fit with the full range of field measured viscosities, giving three-phase mixture viscosities, upon eruption, of 110–140 Pa s (5% crystals, no bubble effect due to sheared vesicles) to 850–1400 Pa s (25–30% crystals, 40–60% spherical vesicles). The ability of the three-phase treatment to characterize the full range of melt-crystal-bubble mixture viscosities in both settings indicates the potential of this method in characterizing basaltic lava mixture viscosity.

1. Introduction

A basaltic lava is a three-phase mixture comprising a fluid component (basalt) plus voids (bubbles and/or space opening along shear lines) and solids (crystals, both phenocrysts and microphenocrysts). This mixture plays an influential role in determining the bulk rheology of the flow [e.g., *Pinkerton and Stevenson*, 1992; *Crisp et al.*, 1994; *Cashman et al.*, 1999]. Derivation of viscosity is crucial in applications that seek to use field data and measurements such as lava flow temperature, crystallinity, and vesicularity for calculation of the bulk rheology of different suspensions [e.g., *Crisp et al.*, 1994; *Pinkerton and Norton*, 1995; *Cashman et al.*, 1999; *Bagdassarov and Pinkerton*, 2004], and/or to model lava flow dynamics [e.g., *Dragoni*, 1989; *Ishihara et al.*, 1990; *Harris and Rowland*, 2001].

Many rheological treatments exist for one- and two-phase magma and/or lava mixtures. Single-phase treatments obtain fluid viscosity from composition, water content, and/or temperature [e.g., *Shaw*, 1969; *Bottinga and Weill*, 1972; *Giordano and Dingwell*, 2003]. In addition, two-phase treatments have been applied to mixtures of fluid and crystals [e.g., *Marsh*, 1981; *Pinkerton and Stevenson*, 1992; *Costa*, 2005; *Sato*, 2005] or fluid and bubbles [e.g., *Manga et al.*, 1998, *Rust and Manga*, 2002; *Pal*, 2003; *Llewellin and Manga*, 2005]. *Dobran* [1992] and *Papale and Dobran* [1994], consider the three-phase viscosity for

magma ascending a conduit during explosive Plinian eruptions. Nevertheless, three-phase treatments have received less attention in the context of lava flows. Three-phase treatments have been developed in other contexts such as in the study of suspensions and multiphase flow [e.g., *Phan-Thien and Pham*, 1997]. In this paper, we examine the use of the three-phase treatment of *Phan-Thien and Pham* [1997] for a basaltic lava mixture. This rigorously derived treatment reduces, in a limiting case, to a viscosity treatment of rigid spheres and fluid. This formulation has good agreement with experimental data and is comparable to established formulae for two-phase systems currently in use for lava, i.e., treatments based on the work by *Einstein* [1906] and *Roscoe* [1952].

In assessing one-, two-, and three-phase treatments of lava flow viscosity we consider two cases for which independent measurements of viscosity are available. These allow for appraisal of the applicability of each method to basaltic mixtures. Our two cases are taken from the 1984 eruption of Mauna Loa (Hawaii), for which viscosity measurements are available from *Moore* [1987], and lava at Mount Etna (Italy) measured using a viscometer by *Pinkerton and Sparks* [1978] in 1975.

2. The 1984 Mauna Loa and 1975 Mount Etna Lavas

Both the 1984 eruption of Mauna Loa and 1975 eruption of Mount Etna provide excellent test cases for two reasons. First, there are sufficient published composition, temperature, crystallinity and vesicularity data to allow application of existing one-, two-, and three-phase viscosity treatments. Second, independent viscosity measurements allow the results of these treatments to be assessed.

2.1. Mauna Loa 1984

The 1984 eruption of Mauna Loa began on 25 March, continued for 21 days until 14 April, and was characterized by emplacement of channel-fed flows extending up to 27 km from the vent at discharge rates of up to 280 m^3 s^{-1} [*Lipman and Banks*, 1987]. Measurements by *Lipman and Banks* [1987] give eruption temperatures within a fairly narrow range (1140 ± 3°C) throughout the eruption. Lava densities, however, decreased from 1000 to 1200 kg m^{-3} during the first 12 days to 400–800 kg m^{-3} thereafter [*Lipman and Banks*, 1987]. For a dense rock density of 2600 kg m^{-3}, this equates to an increase in vesicularity from 55–60% to 70–85%. At the same time, crystallinities increased from 0–5% on 25 March to 10–15% by 26–28 March. By 29 March to 9 April crystallinities were 15–25%, increasing to 25–30% during 10–15 April [from *Lipman and Banks*, 1987, Figure 57.25]. Calculations of lava viscosity were made by *Moore* [1987] using measured flow velocity with channel width and depth data from the same sample stations as used by *Lipman and Banks* [1987]. *Moore*'s [1987] data revealed an increase in at-vent lava viscosity from 140–160 Pa s during 2–4 April, to 270–450 Pa s by 8–9 April, reaching 900–1400 Pa s by 12–13 April. The increase in crystallization was suggested to have caused the synchronous increase in effective viscosity [*Lipman et al.*, 1985], thereby defining three viscosity-crystallinity phases (Table 1). At the same time, major element compositions for the lava were obtained by *Rhodes* [1988] and showed the lava to have an extremely homogeneous whole rock composition with an average silica content of 52.3 wt % (Table 2), with a calculated H_2O content for the residual melt at the surface of 0.1 wt % [*Russell*, 1987]. Using this average composition in the MELTS model of *Ghiorso and Sachs* [1995], we expect a liquidus temperature of ~1200°C.

2.2. Etna 1975

The 1975 effusive eruption of Mount Etna began on 24 February from a vent located 2.5 km north of the summit and fed by a radial fissure extending from the summit area [*Pinkerton*

and Sparks, 1976]. Low effusion rate (0.3–0.5 $m^3 s^{-1}$) activity continued until mid-September, when summit activity resumed [*Pinkerton and Sparks*, 1976]. Erupted lavas had phenocryst contents of 50–60%, core temperatures of 1070–1090°C and vesicularities of 10–20% [*Pinkerton and Sparks*, 1976]. These values are typical of Etnean lavas, which are porphyritic, having phenocryst contents of 30–40% [e.g., *Tanguy*, 1973; *Armienti et al.*, 1984, 1994a], with vesicularities of ~20% [*Herd and Pinkerton*, 1997]. Core temperatures vary with distance from vent [*Pinkerton and Sparks*, 1976], but near-vent measurements are typically in the range 1060–1125°C [e.g., *Tanguy*, 1973; *Calvari et al.*, 1994], with a range of 1043–1111°C being obtained from MgO geothermometry [*Pompilio et al.*, 1998].

Measurements of the 1975 lava were made by *Pinkerton and Sparks* [1978] using a viscometer at a site 3 m down flow from an active vent and at a depth of 0.2 m. The core temperature at the time of measurement was 1086 ± 3°C and lava crystallinity was 45% [*Pinkerton and Sparks*, 1978]. The measured viscosity of 9400 ± 1500 Pa s compares with 3000–38,000 Pa s obtained by *Walker* [1967] and 5000–74,000 given by *Tanguy* [1973] on the basis of channel dimension and flow velocity measurements during Etna's 1966 eruption. *Gauthier* [1973] also used a viscometer to obtain viscosities in the range 10^3–10^5 Pa s during Etna's 1971 eruption, and *Calvari et al.* [1994] obtained 8000–19,000 Pa s using channel dimension and velocity estimates for lava within a few kilometers of the 1991–1993 vent. The estimates of *Calvari et al.* [1994] increased to a maximum of 2×10^5 Pa s at greater distances. Given the simultaneous measurement of temperature and crystallinity by *Pinkerton and Sparks* [1978], and at-vent conditions (i.e., minimal posteruption cooling, crystallization and degassing), we use this as a test case for our subsequent modeling.

Lava erupted from Mount Etna during 1966–1993 was alkaline basalt to basaltic Hawaiite in composition [*Armienti et al.*, 1984; *Tanguy and Clocchiatti*, 1984], with typical SiO_2 contents of 47–49 wt % (Tables 3 and 4). Using these average compositions in MELTS, we obtain a liquidus temperature of 1160°C. Prior to degassing, the most primitive melts at Etna contain up to 3.4 ± 0.2 wt % H_2O [*Métrich et al.*, 2004; *Spilliaert et al.*, 2006]. However, degassing during ascent causes H_2O content to decrease substantially, so that matrix glasses usually contain <0.2–0.35 wt % H_2O [e.g., *Metrich and Clocchiatti*, 1989; *Metrich et al.*, 1993; *Spilliaert et al.*, 2006], where slow ascent and shallow storage will result in a more thoroughly degassed magma. Following the data of *Tanguy* [1973] for the 1967 summit eruption (Table 3), we select a H_2O content of 0.1 wt % for summit lavas, which we assume have undergone slower ascent and longer storage times than lavas erupted during flank eruptions. For faster ascending magma involved in flank eruptions higher values may be more appropriate [e.g., *Métrich et al.*, 2004], where the value of 0.4 wt % obtained for the 1971 flank eruption by *Tanguy* [1973] (Table 3) compares with ~0.5 wt % for lava erupted during the 1991–93 flank eruption [*Armienti et al.*, 1994a].

3. Review of Existing One- and Two-Phase Treatments of Basaltic Mixtures

3.1. One-Phase Treatment: Fluid Phase Viscosity

The viscosity of the fluid phase of the lava mixture can be calculated as a function of composition [e.g., *Bottinga and Weill*, 1972], temperature [e.g., *Shaw*, 1969] and/or water content [e.g., *Shaw*, 1972].

At supraliquidus temperatures we assume a one-phase (fluid only) system. Following *Bottinga and Weill* [1972], at supraliquidus temperatures, Newtonian viscosity of the fluid (η_f) can be calculated from lava composition using an Arrhenius mixture rule:

$$\ln(\eta_f) = \sum X_i D_i, \quad (1)$$

where X_i is the mole fraction of the ith component and D_i is a temperature- and compositional-dependent constant obtained from tables of *Bottinga and Weill* [1972].

Fluid phase viscosity can also be calculated as a function of temperature (T). Given constant composition and no crystallization, variation in η_f with T obeys an Arrhenius relation given by

$$\eta_f(T) = A \exp^{(B/T)}, \quad (2)$$

in which A is a constant set equal to the fluid viscosity at an arbitrary reference temperature and B is a measure of the energy required to activate viscous flow. Such a relationship was apparent in data for Hawaiian tholeiite [*Shaw*, 1969] and for Etnean lavas [*Gauthier*, 1973] (Figure 1). While *Shaw* [1969] gives A of 4.8×10^{-7} Pa s and B of 26500 K^{-1} for the tholeiitic melt of the Makaopuhi lava lake (Kilauea), values of 3.1×10^{-9} Pa s and 31690 K^{-1} were obtained for Etna (1971 lavas) from data in *Gauthier* [1973] by *Chester et al.* [1985].

Below liquidus, crystallization causes the fluid composition to change and non-Newtonian effects to become apparent [*Gauthier*, 1973; *Ryerson et al.*, 1988]. Consequently viscosity begins to increase at a faster rate with decreasing temperature, so that equation (2) no longer applies (Figure 1). Instead, $\eta_f(T)$ can be described by

$$\eta_f(T) = \eta_0 \exp^{C(T0-TL)}, \quad (3)$$

in which η_0 is viscosity at liquidus temperature (T_0), C is a constant and T_L is the below liquidus lava temperature. For Hawaiian tholeiitic samples, *Shaw* [1969] gives C of 0.02 K^{-1}, whereas *Dragoni* [1989] uses 0.04 K^{-1} for Etna (Figure 1).

The commonly used approach of *Shaw* [1972] extends that of *Bottinga and Weill* [1972] adding the effect a water component. This approach also allows fluid viscosity to be calculated as a function of composition and temperature:

$$1n(\eta_f) = s(10^4/T) - s\, c_T + c_\eta, \quad (4)$$

in which s is the characteristic slope for the viscosity-temperature relationship of a given multicomponent mixture and c_T are c_η temperature- and viscosity-dependent constants. Calculation of each of these coefficients can be achieved following *Shaw* [1972].

All of the above approaches assume Arrhenian temperature dependence for viscosity. However, this assumption may not be valid such that non-Arrhenian dependences, empirically derived from experimental data, may be more appropriate [e.g., *Hess and Dingwell*, 1996]. *Giordano and Dingwell* [2003] provide such a non-Arrhenian relation for Etnean lavas using experimental data derived from dry and hydrated 1992 Etna alkali basalt:

$$\mathrm{Log}_{10}\eta_f = -4.643 + [5812.44 - 427.04 \times H_2O] / [T(K) - 499.31 + 28.74 \times \ln(H_2O)], \quad (5)$$

in which H_2O is the water content in wt % (Figure 2). Likewise, *Whittington et al.* [2000] provide an empirically derived non-Arrhenian relationship for tephrite (50.6 wt % SiO_2).

3.2. Two-Phase Treatment: Fluid and Crystals or Bubbles

Existing two-phase treatments applied to magma and lava allow us to assess either the effect of crystals [e.g., *Pinkerton and Stevenson*, 1992; *Costa*, 2005] or bubbles [e.g., *Manga et al.*, 1998; *Pal*, 2003] on the mixture viscosity, but not both.

Variation of a fluid-crystal mixture viscosity with crystal content can be described by the Einstein-Roscoe relationship [*Einstein*, 1906; *Roscoe*, 1952; *Shaw*, 1969; *Ryerson et al.*, 1988]:

$$\eta(\varphi) = \eta_f(1 - R\varphi)^{-2.5}, \quad (6)$$

in which φ is the particle (crystal) concentration and R is $1/\varphi_{max}$, φ_{max} being the maximum concentration that can be attained by the particles. For magma, R of 1.67 has been proposed [*Marsh*, 1981], which corresponds to a particle concentration of 60% at which the suspension viscosity has infinite viscosity [*Pinkerton and Stevenson*, 1992]. *Pinkerton and Stevenson* [1992] argued that *Marsh*'s [1981] relationship provides a useful approximation for magmas at low crystal contents and strain rates, but expressed reservations on the universal acceptance of equation (6). Moreover, for high-particle-concentration suspensions the viscosities at low and high strain rates may differ considerably. *Pinkerton and Stevenson* [1992] proposed the use of the relationship defined by *Gay et al.* [1969] for high strain rates:

$$\eta(\varphi) = \eta_f \exp\left\{\left[2.5 + (\varphi/(\varphi_{max} - \varphi))^{0.48}\right]\varphi/\varphi_{max}\right\}. \quad (7)$$

Pinkerton and Stevenson [1992] also question a universal acceptance of 60% as a reasonable value for φ_{max}, where φ_{max} will probably vary for most lavas. Although the range will not be that great, *Pinkerton and Stevenson* [1992] point out that *Marsh* [1981] considers a range of 50–70% to be realistic. This yields likely R in the range 1.4 to 2; where we plot the equation (6) relationship for φ_{max} of 70 (R = 1.4) and 50% (R = 2) in Figure 3.

Variation of a fluid-bubble mixture viscosity with bubble content can also be described by the Einstein-Roscoe relationship where, for a suspension of spheres [*Roscoe*, 1952],

$$\eta(\varphi_b) = \eta_f(1 - 1.35\varphi_b)^{-2.5} \quad (8)$$

φ_b being the bubble concentration. In this formulation the maximum bubble packing concentration (φ_{bmax}) must be 0.74, i.e., $1/\varphi_{bmax} = 1.35$. However, changes in bubble content can serve to both increase and decrease the mixture viscosity depending on bubble shape. While bubbles that remain spherical will increase the mixture viscosity, deformed (sheared) bubbles will reduce the viscosity because their elongated shape allows for sliding

motion [*Manga et al.*, 1998]. This effect was noted for pahoehoe by *Keszthelyi and Self* [1998]. While flows with <20% bubbles required significant effort to stir with a hammer, flows with >50% (and presumably sheared) bubbles offered minimal resistance [*Keszthelyi and Self*, 1998]. In contrast, the emplacement style of near-crystal-free pahoehoe lobes on Kilauea can only be explained by the presence of (nonsheared) spherical bubbles. The presence of such a bubble population is necessary to increase the required bulk viscosity by a factor of ~100 from the bubble-free state [*Gregg and Keszthelyi*, 2004].

Because bubbles can serve to decrease or increase bulk viscosity, depending on strain rate, *Pal* [2003], for example, favors two forms of equation (8):

$$\eta(\varphi_b)=\eta_f\left[1-(\varphi_b/\varphi_{bmax})\right]^{-\varphi bmax} \tag{9a}$$

for regimes in which the bubbles are spherical, and

$$\eta(\varphi_b)=\eta_f\left[1-(\varphi_b/\varphi_{bmax})\right]^{5\varphi bmax/3} \tag{9b}$$

in cases where the bubbles are sheared. For *Pal* [2003], a value of 0.7 for φ_{bmax} yielded reasonable results.

However, as with the maximum crystal content, assigning a value for φ_{bmax} is problematic. For the 1984 Mauna Loa lava, for example, *Lipman and Banks* [1987, p. 1550] obtain maximum bubble contents of 85% and describe near-vent lava as “fluffy near-reticulite” with “the consistency of whipped egg white.” This is in agreement with our own measurements on similar textured lava flows erupted from the Pu'u 'O'o vent of Kilauea (Hawaii) during 1998 which have maximum bubble contents of 80–90% (A. J. L. Harris, unpublished data, 2003). As a result, *Llewellin and Manga* [2005] argue that the most reasonable course is to set φ_{bmax} to 1. This means that equations (9a) and (9b) reduce to:

$$\eta(\varphi_b)=\eta_f\left[1-\varphi_b\right]^{-1} \tag{10a}$$

and

$$\eta(\varphi_b)=\eta_f\left[1-\varphi_b\right]^{5/3}. \tag{10b}$$

Equation (10a) was initially proposed by *Taylor* [1932] to describe the viscosity of a dilute mixture with spherical bubbles. *Manga and Loewenberg* [2001] thus refine the relationship further to

$$\eta(\varphi_b)=\eta_f\left[1+f\varphi_b\right], \tag{11}$$

f being a constant that depends on the properties of the suspended bubbles, as given by the capillary number, with *f* having a value of 1 for spherical bubbles and −1.67 for highly

sheared bubbles. The relationships defined by equations (8) and (10) are plotted, with field data, in Figure 4.

4. Application of One- and Two-Phase Treatments of Basaltic Mixtures

4.1. Mauna Loa, 1984: One-Phase-Fluid (Melt) Viscosity

The viscosity of the fluid phase at liquidus can be assessed using the melt composition and liquidus temperature (T_{liquid}) in equations (1), (2), and/or (4). For Mauna Loa's 1984 lava, the whole rock analyses of *Rhodes* [1988], with T_{liquid} of 1200°C and water content of 0.1 wt % [*Russell*, 1987], yields η_f of ~40 Pa s at liquidus. The methodologies of *Bottinga and Weill* [1972] and *Shaw* [1972] give similar ranges of 35–38 and 41–44 Pa s, respectively (Table 2). These values compare with 31 Pa s using the supraliquidus temperature-dependent relationship of *Shaw* [1969] with a temperature of 1200°C (equation (2)). We thus expect a viscosity of the melt phase of Mauna Loa magma, upon eruption, of 30–40 Pa s. Higher precrystallization water contents of ~1 wt% [*Russell*, 1987] may reduce the supraliquidus viscosity further, the presence of water serving to depolymerize the melt by breaking up the Si-O-Si bridging bonds due to formation of Si-O-H nonbridging bonds. For the whole rock compositions of Table 2, with 1 wt % H_2O, the approach of *Shaw* [1972], for example, gives a minimum bound on viscosity for Mauna Loa's undegassed, crystal-free melt of ~20 Pa s.

At subliquidus temperatures, crystallization will cause the composition of the remaining fluid to evolve, so that recalculation of η_f to take into account the new composition and temperature of the interstitial fluid is necessary [*Getson and Whittington*, 2007]. In the case of the Mauna Loa 1984 lava, although the eruption temperature and bulk composition remained close to the average throughout the entire eruption, increases in crystallization caused glass compositions to evolve, so that they decreased slightly in MgO and CaO and increased in TiO_2 and K_2O [*Rhodes*, 1988]. Thus, although the calculated fluid viscosity on the basis of eruption temperature (1140°C) and whole rock composition remained stable, the fluid viscosity calculated from the glass composition increased (Table 2). Our glass-composition-based calculations based on the work by *Bottinga and Weill* [1972] and *Shaw* [1972] are in reasonable agreement giving fluid viscosities at 1140°C of 120–130 and 90–100 Pa s, respectively, during the opening (low crystallinity) phase. This increases to ~150 Pa s (following *Bottinga and Weill* [1972]) or ~125 Pa s (following *Shaw* [1972]) for the closing (high crystallinity) phase (Table 2). The viscosity of the fluid phase would therefore have increased, as the composition evolved, from ~100 Pa s (during the opening phase) to ~125 Pa s (by the closing phase). Using these fluid viscosities in the two-phase treatments, we can now assess the mixture (fluid plus crystals or bubbles) viscosity as a function of crystal or bubble contents.

4.2. Mauna Loa, 1984: Two-Phase–Fluid-Crystal Mixture Viscosity

To estimate the bulk viscosity of the fluid-crystal mixture, we apply equations (6) and (7) with an opening phase fluid viscosity of 100 Pa s and a closing phase fluid viscosity of 125 Pa s (Figure 3 and Table 1). Application of equations (6) and (7) with the maximum expected maximum crystal content (φ_{max}) of 70% produces a fit only for the intermediate-viscosity phase crystallinities. Application of equations (6) and (7) with the minimum expected maximum crystal content (φ_{max}) of 50% provides a fit using the intermediate-viscosity phase crystallinities and the high-viscosity phase crystallinities. However, estimates during the low-viscosity phase remain too high (Figure 3 and Table 1).

Crisp et al. [1994], following a similar approach, obtained 210–300 Pa s for near-vent fluid-crystal mixtures. They proposed that about 2 April (when measured viscosities were lowest) the near agreement with *Moore's* [1987] values indicated that the effect of bubbles on the

mixture viscosity was negligible. In fact the presence of sheared bubbles in the fast moving channelized lava may have lowered the bulk viscosity, perhaps accounting for the factor of two difference with *Moore's* [1987] estimate of 140–160 Pa s [*Crisp et al.*, 1994]. In agreement with our results (Figure 3 and Table 1), *Crisp et al.* [1994] also found it difficult to attribute the final increase in viscosity recorded by *Moore* [1987] to 900–1400 Pa s solely to increased crystallinity. Instead they argued that increased bubble contents and decreased shear rates were now causing unsheared (spherical) bubbles to force the mixture viscosity upward.

4.3. Mauna Loa, 1984: Two-Phase–Fluid-Bubble Mixture Viscosity

We can assess the effects of adding bubbles to a two-phase fluid-bubble mixture using equations (8), (10a), and (10b). As suggested by *Crisp et al.* [1994], equation (10b) indicates that the effect of adding highly sheared bubbles to a fluid-bubble mixture will decrease the mixture viscosity by a factor of 3.2 to 7.4 given bubble contents of 50 to 70% (Figure 4a). However, using a two-phase fluid-bubble mixture we can only fit the data of *Moore* [1987] if we use equation (10a). This, appropriately, is the model for a dilute mixture with spherical bubbles. We note, though, that we are still only able to obtain a fit with the intermediate-viscosity phase measurements (Figure 4a).

Thus, viscosity changes documented at Mauna Loa are difficult to explain using a two-phase model that considers a mixture comprising solely fluid and crystals or fluid and bubbles. A treatment taking into account the presence of crystals in a three-phase mixture also containing bubbles seems, though, entirely capable of yielding results that would agree with those of *Moore* [1987].

4.4. Etna 1975: One-Phase–Fluid (Melt) Viscosity

The whole rock analyses for Etnean lavas given in Table 3, with water contents of 0.1–0.4 wt %, yields fluid phase viscosities (at liquidus, T_{liquid} = 1160°C) of 20–60 Pa s. Application of the method of *Bottinga and Weill* [1972] gives a tighter, and slightly lower, range of 16–27 Pa s than that obtained from *Shaw* [1972] of 20–57 Pa s (Table 3). The spread in both sets of values results from slight compositional differences between each eruption. This is exaggerated in our application of *Shaw* [1972] due to our use of 0.1 wt % H_2O for summit eruptions and 0.4 wt % for flank eruptions. The summit eruptions of 1972, 1975, and 1980, for example, involved slightly more evolved compositions than the flank eruptions of Table 3. This appears consistent with our use of a more degassed water content for these summit eruptions. As a result, the range of η_f for the summit eruptions is 19–27 Pa s (following *Bottinga and Weill* [1972]), or 40–57 Pa s (following *Shaw* [1972]). This compares with 17–22 and 20–30 Pa s obtained when applying the two methodologies with the Table 3 flank eruption compositions. Being insensitive to compositional variation, supraliquidus fluid viscosity derived from the temperature-dependent relationship of equation (2) is the same for all cases, and somewhat low, at 12 Pa s. This value is set by our use of a T of 1160°C in equation (2) for calculation of viscosity at liquidus (i.e., T = T_{liquid} = 1160°C).

For a melt temperature of 1160°C, application of *Giordano and Dingwell* [2003] (equation (5)) gives 102 and 38 Pa s for H_2O contents of 0.1 and 0.4 wt %, respectively. Being set specifically for an Etnean basalt (1992 lava with 47.03 wt % SiO_2) this should give the most realistic result and is comparable to the upper ranges obtained from *Shaw* [1972] using the Table 3 summit and flank compositions with water contents of 0.1 and 0.4 wt %. Given undegassed water contents of 3.4 wt % [*Métrich et al.*, 2004; *Spilliaert et al.*, 2006], with the whole rock compositions of Tables 3 and 4, *Shaw* [1972] gives a minimum viscosity for

Etnean melt, prior to ascent and degassing, of 3–9 Pa s. This compares with ~1 Pa s obtained from *Giordano and Dingwell* [2003] (Figure 2).

At subliquidus temperatures, crystallization causes the melt composition to evolve so that SiO_2 contents of 50–52 wt % are more appropriate when considering the fluid viscosity at eruption temperature and melt composition (Table 4). Given an eruption temperature of 1080°C and water content of 0.4 wt %, the two Table 4 compositions yield a much wider spread of possible melt viscosities than at subliquidus. While our approach based on the method of *Bottinga and Weill* [1972] gives η_f of 662 and 466 Pa s for the two lavas, respectively, *Shaw* [1972] gives 201 and 218 Pa s. Decreasing the water content used by *Shaw* [1972] to 0.1 wt % increases these values to 272 and 296 Pa s. Being based on more evolved compositions, these glass-composition-derived values are typically higher than sub-liquidus η_f obtained at 1080°C using the whole rock compositions of Tables 3 and 4. This is especially true of the derivations based on the method of *Shaw* [1972]. The purely temperature-dependent approach gives a constant value (defined by our use of T_L = 1080°C in equation (3)) of 305 Pa s. This is midway between the two ranges obtained using the methods of *Bottinga and Weill* [1972] and *Shaw* [1972]. A question thus arises with respect to the proper choice for the subliquidus melt viscosity.

For the lava temperature of 1086 ± 3°C measured by *Pinkerton and Sparks* [1978], application of the work by *Giordano and Dingwell* [2003] gives 135 ± 10 Pa s (for 0.4 wt % H_2O) and 425 ± 30 Pa s (for 0.1 wt % H_2O). These bound the wide spread of subliquidus melt viscosities given in Table 4 (Figure 5). The two values thus appear appropriate for melt viscosity, upon eruption at 1086°C, of (1) relatively undegassed Etnean melt, and (2) well-degassed, slightly evolved, Etnean melt, respectively. An absolute minimum η_f of ~40 Pa s is expected for water contents of 1.0 wt %, with a maximum of ~2200 Pa s for completely degassed lava (<0.01 wt % H_2O) (Figure 5).

4.5. Etna 1975: Two-Phase–Fluid-Crystal Mixture Viscosity

Given the degassed fluid viscosity of 425 ± 30 Pa s, application of equation (7), the high strain rate formulation, with φ_{max} of 60%, provides an excellent fit with the field data (Figure 6a). The 45% crystal content yields a calculated viscosity for the fluid-crystal mixture of 9900 ± 700 Pa s, matching the 9400 ± 1500 Pa s measured by *Pinkerton and Sparks* [1978]. However, while application of Einstein-Roscoe (equation (6)) provides an overestimate, use of the undegassed fluid viscosity (135 ± 10 Pa s) provides an underestimate. Use of φ_{max} of 50 and 70% also provides overestimates and underestimates of the mixture viscosity, respectively (Figure 6).

The good results obtained using equation (7) with η_f = 425 ± 30 Pa s and φ_{max} = 60% may indicate that, in this case, the influence of bubbles on the mixture rheology was negligible, so that mixture viscosity can be described by the high strain rate formulation for a fluid-crystal mixture of equation (7). In addition, it appears to indicate that use of 425 ± 30 Pa s to describe the fluid viscosity of degassed, slightly evolved, summit lavas at Etna is appropriate. The whole rock analyses of *Armienti et al.* [1984] show the 1975 summit lavas as having a slightly more evolved composition in respect to the flank eruptions (Table 3). However, we note that *Armienti et al.* [1994a], when using the 1991–1993 lava compositions and water content from *Shaw* [1972] and correcting for crystal content using Einstein-Roscoe, arrived at a liquid-crystal mixture viscosity of ~1250 Pa s; an order of magnitude less than the 8000–19,000 Pa s range obtained for the same flows by *Calvari et al.* [1994] using the Jeffreys equation.

Although use of φ_{max} = 60% in our best fit (Figure 6a) follows that proposed by *Marsh* [1981], and lies midway within the likely range of 50–70%, use of this φ_{max} is a

considerable assumption [*Pinkerton and Stevenson*, 1992] as is the negligible effect of bubbles. Other solutions using φ_{max} of 50 and 70% do provide fits which are close, but which overestimate and underestimate, respectively, the measured viscosity (Figures 6). It is thus entirely possible that the influence of a population of spherical bubbles in a three-phase (fluid-crystal-bubble) mixture could increase the viscosity of that mixture viscosity further, allowing a fit in cases which currently underestimate the measured value. This could allow a fit using the high-viscosity regime with φ_{max} = 70% (Figure 6a). Alternatively, a population of sheared bubbles may decrease the three-phase mixture viscosity allowing a fit in cases which currently overestimate the measured value. This could allow a fit using with φ_{max} = 50% (Figure 6b).

4.6. Etna 1975: Two-Phase–Fluid-Bubble Mixture Viscosity

The bubble content of the 1975 Etna lava was not trivial, being 10–20% in the crust alone [*Pinkerton and Sparks*, 1976]. Near-vent measurements for pahoehoe and 'a'a at Etna give core vesicularities of 25–35% [*Herd and Pinkerton*, 1997]. Although none of the formulations plotted in Figure 4b provide a fit with the field data, with all yielding underestimates for the two-phase (fluid-bubble) mixture viscosity, they do show how populations of sheared versus spherical bubbles can significantly change the mixture viscosity of a fluid-bubble system. A three-phase treatment is thus needed for consideration of the effects of bubble population as well as crystal constant on the mixture viscosity.

5. Application of the Three-Phase Treatment

Phan-Thien and Pham [1997] introduce a treatment for the viscosity of a three-phase mixture comprising a suspension of rigid spheres and bubbles. In this treatment suspension viscosity is obtained from a differential scheme that allows for the addition of materials filling up the allowable volume fraction for each phase. From the equation obtained for a suspension of rigid spheres and bubbles in the same size range, expressions for viscosity may be formulated for cases in which one phase has a much larger size than the other. If one phase is much smaller in relative size than the other, it may be treated as an effective medium along with the base fluid viscosity. Within this approximation, the expressions for crystals smaller than bubbles (and visa versa) can be found, with the treatment simplifying to three cases, in which v_c and v_b are the crystal and bubble volume fractions, respectively. The three cases are as follows:

In case 1, crystals are smaller than bubbles,

$$\eta(\varphi, \varphi_b,) = \eta_f [1 - v_c/(1 - v_b)]^{-5/2}(1 - v_b)^{-1}. \quad (12a)$$

In case 2, crystals and bubbles are of the same size range,

$$\eta(\varphi, \varphi_b,) = \eta_f (1 - v_c - v_b)^{-(5vc+2vb)/2(vc+vb)}. \quad (12b)$$

In case 3, crystals are larger than bubbles,

$$\eta(\varphi, \varphi_b,) = \eta_f [1 - v_b/(1 - v_c)]^{-1}(1 - v_c)^{-5/2}. \quad (12c)$$

We note that the mixture viscosity increases less rapidly with crystal content such that for any given crystal content, mixture viscosity will be highest for case 1 and lowest for case 3 (Figure 7). Moreover, in the limiting case of $v_b = 0$, the expression for rigid spheres obtained by *Roscoe* [1952] is recovered, so that all cases represented by equations (12a) to (12c) reduce to equation (6) with a φ_{max} of 100%. Likewise, for $v_c = 0$, an expression for a bubble suspension as described by *Batchelor* [1970] is found. The reader is referred to *Phan-Thien and Pham* [1997] for further details of this treatment.

These expressions allow for assessment of the mixture viscosity as a function of crystals and bubbles. For example, the three-phase treatments provide good fits with the Mauna Loa phase 2 and 3 viscosities and crystallinities given bubble volume fractions of 0.3 and 0.5, respectively (Figure 7a). The three-phase treatment is also able to fit with the low-viscosity phase data if used with a bubble content of zero, i.e., bubbles have no effect on the mixture viscosity. For Etna, using the three-phase models with the maximum expected bubble volume fraction (0.35) provides a good fit if the 425 Pa s melt viscosity (for a degassed Etnean lava) is used (Figure 7b). As argued in the two-phase discussion, this is reasonable given that these were evolved, degassed, summit lavas.

Applying the three-phase treatments thus allows us to assess those modeled scenarios that provide the best fit with the field data. At Mauna Loa and Etna crystals and bubbles span a range of sizes, where the crystals can be both larger and smaller than the bubbles. For the Mauna Loa 1984 flow crystals ranged in size up to a maximum of 0.012 cm, with an average size of 0.005 cm [*Crisp et al.*, 1994]. This compares with mean bubble sizes obtained for Kilauea lava samples by *Cashman et al.* [1999] of 0.025–0.15 cm. For Etna, crystal sizes in the range 0.001–0.15 cm [*Armienti et al.*, 1994b] compare with bubble sizes in the range 0.01–0.35 cm [*Herd and Pinkerton*, 1997]. Given the variety of crystal and bubble sizes we are unable to assign a specific case. Thus, we use cases 1 (equation (12a)) and 3 (equation (12c)) as end-member models.

For Mauna Loa (Figure 8), these models provide good fits with the low-viscosity phase (phase 1) data if the bubbles had no effect (i.e., shearing meant that they had little-to-no influence on the viscosity of the mixture). The phase 2 and 3 data can be modeled with the case 1 treatment (Figure 8a) using vesicularities of 15–40 and 40–55%, respectively, with the fits being similar if we use the low-viscosity melt of the opening phase or the higher viscosity melt of the closing phase (Figure 8a). Applying the case 3 model (Figure 8b) allows us to obtain fits at slightly higher vesicularities of 20–50% (for phase 2) and 50–65% (for phase 3). Although these vesicularities are a little lower than those obtained from the density data of *Lipman and Banks* [1987], they do show a fit with the field data in that vesicularities increased from moderate levels during phase 2 to high levels in phase 3, a change that was recorded in the field. Thus, for Mauna Loa, the three-phase treatment is the only treatment that can reproduce the full viscosity history using plausible input for each of the three eruption phases. This suggests that the change in viscosity witnessed during the 1984 Mauna Loa eruption was a function of the change in both crystal and bubble content, with evolution of the melt playing a minor-to-insignificant role.

At Etna, we first use the fluid viscosity appropriate for a summit eruption of degassed lava (425 Pa s) in the three-phase treatments (Figure 9). We obtain a fit with the field data using the case 1 model for vesicularities in the range 25–35%, this range giving (for $v_c = 0.45$) a mixture viscosity of 5600–12,500 Pa s (Figure 9a). While this vesicularity range spans a plausible vesicularity range for Etna, the output viscosity compares well with the field measurement of 9400 ± 1500 Pa s indicating that this (case 1) three-phase treatment can reproduce plausible viscosities for Etna. However, application of the case 2 model only produces a fit for vesicularities of 40–45% (Figure 9b). This is a little on the high side for an

Etnean lava, thus case 1 appears more appropriate for Etna suggesting a scenario where crystals are smaller than the bubbles. This seems consistent with the crystal and bubble data of *Armienti et al.* [1994b] and *Herd and Pinkerton* [1997], respectively, which indicate the bubbles occupying a higher size range than the crystals. Using the lower fluid viscosity of 135 Pa s, we only obtain fits at unrealistically high vesicularities of 40–55% (Figure 10). Once more, this indicates that the use of the higher fluid viscosity for a degassed, slightly more evolved melt is appropriate for this case.

6. Conclusion

Differences in lava composition, water content, temperature, crystallinity and vesicularity control variations in the viscosity of the erupted mixture. While eruption of more evolved basaltic melt forces mixture viscosity upward, any increases in water content drives viscosity downward by depolymerizing the melt. Generic, Arrhenius relations are available allowing for calculation of melt from composition [*Bottinga and Weill*, 1972] or composition, water content and temperature [*Shaw*, 1972]. More accurate, case-specific, empirically derived relations allow water and temperature based estimates specific to a particular composition [e.g., *Giordano and Dingwell*, 2003]. Two-phase formulations have commonly been applied to examine the viscosity of fluid-crystal and/or fluid-bubble mixture. These show that increased crystal and bubble content can push the mixture viscosity upward in the case of a spherical bubble population. However, the presence of a sheared bubble population can reduce the mixture viscosity. These two-phase treatments, though, are unable to model the full range of viscosities measured at Mauna Loa and Etna, a result which suggests that one of the phases has not been properly included. The three-phase treatment of *Phan-Thien and Pham* [1997] is capable of simulating the full range of viscosities resulting from variations in crystal and bubble content if applied within appropriate limits.

For subliquidus (eruption) temperatures (~1140°C), melt viscosities calculated, following *Bottinga and Weill* [1972] and *Shaw* [1972], for Mauna Loa's tholeiitic basalt are in reasonable agreement, giving values of 115–150 Pa s and 80–125 Pa s, respectively, though we note that the method of *Bottinga and Weill* [1972] is only applicable down to 1200°C. Thus, for temperatures below 1200°C, *Bottinga and Weill* [1972] must be input into a subliquidus temperature-dependent model (e.g., equation (3)) to obtain an appropriate fluid viscosity at the eruption temperature. This allows the calculation of melt viscosities which cross-check with *Shaw* [1972]. In the case of Mauna Loa, the melt was largely degassed with respect to water (≤0.1 wt % H_2O), which likely facilitated the match. Slight variations in composition caused the mixture viscosity to vary by ~25%. Two-phase models show that increases in the crystal or spherical bubble content could force the mixture viscosity for Mauna Loa's lava upon eruption to 1200 Pa s (for a crystal content of 30%, no bubbles) or 2000 Pa s (for a spherical bubble content of 50%, no crystals). These values compare with the maximum field-measured value of 1400 Pa s during the final (high crystallinity) phase of the 1984 eruption. Conversely, the presence of a sheared bubble population, in the absence of crystals, may reduce the mixture viscosity to 30–40 Pa s. This value is, however, lower than the minimum field measured value (~140 Pa s) obtained during the opening (low crystallinity) phase of the eruption. Thus, although two-phase treatments can mimic trends measured in the field, they do not always provide good fits with field data. In contrast, the three-phase treatment provides a fit with the full range of field measured viscosities at Mauna Loa (Figure 7a). This indicates three-phase mixture viscosities upon eruption of 110–140 Pa s (5% crystals, no bubble effect due to sheared bubbles) to 850–1400 Pa s (25–30% crystals, 40–60% spherical bubbles). Down-flow cooling, crystallization and bubble evolution will then force these starting values higher with the distance from the vent [e.g., *Moore*, 1987; *Crisp et al.*, 1994].

For Etna we find a much greater difference between melt viscosities calculated following *Bottinga and Weill* [1972] and *Shaw* [1972], with the two approaches giving 390–660 and 50–150 Pa s. In addition, lower water contents and slightly more evolved compositions result from more thorough degassing of some batches, as may be the case during low effusion rate summit eruptions. This will result in higher melt viscosities for the more thoroughly degassed melts. Using a typical eruption temperature of 1080°C with water contents of 0.1 and 0.4 wt % in the empirically derived formulation for Etna's alkaline basalt of *Giordano and Dingwell* [2003] gives 425 ± 30 and 135 ± 10 Pa s, for the two water contents, respectively. Applying the appropriate three-phase model (for a case where crystals are smaller than the bubbles) using the 425 ± 30 Pa s melt viscosity, we obtain a mixture viscosity that compares well with that measured during Etna's 1975 summit eruption by *Pinkerton and Sparks* [1978]. This suggests that the 425 ± 30 Pa s melt viscosity is appropriate to eruptions of degassed lavas at Etna.

The ability of the *Phan-Thien and Pham* [1997] three-phase treatment to characterize the full range of melt-crystal-bubble mixture viscosities at both Mauna Loa and Etna highlights the potential of this formulation in characterizing the mixture viscosity of basaltic lavas. However, the sensitivity of the treatments to input parameters, as well as the assumptions and decisions that need to be made in selecting and applying the appropriate equations, show that to successfully apply the formulations they must be applied with care and with appropriate field data. Appropriate selection of melt temperature and chemistry is first necessary to allow the melt-phase viscosity to be obtained. The sizes and shapes of any crystals and bubbles, as well as degree of bubble shearing, must then be determined so that the appropriate two- and/or three-phase treatment can be applied.

Acknowledgments

We thank Julia Hammer and Alan Whittington for helpful discussions on the viscosity temperature relationships. We also benefited from two thoughtful and careful reviews by an anonymous reviewer and Laszlo Keszthelyi.

References

Armienti P, Barberi F, Innocenti F, Pompilio M, Romano R, Villari L. Compositional variation in the 1983 and other recent Etnean lavas: Insights on the shallow feeding system. Bull Volcanol. 1984; 47:995–1007.10.1007/BF01952357

Armienti P, Clocchiatti R, D'Orazio M, Innocenti F, Petrini R, Pompilio M, Tonarini S, Villari L. The long-standing 1991–1993 Mount Etna eruption: Petrography and geochemistry of lavas. Acta Vulcanol. 1994a; 4:15–28.

Armienti P, Pareschi MT, Innocenti F, Pompilio M. Effects of magma storage and ascent on the kinetics of crystal Growth. The case history of the 1991–93 Mt. Etna eruption. Contrib Mineral Petrol. 1994b; 115:402–414.10.1007/BF00320974

Bagdassarov N, Pinkerton H. Transient phenomena in vesicular lava flows based on laboratory experiments with analogue models. J Volcanol Geotherm Res. 2004; 132:115–136.10.1016/S0377-0273(03)00341-X

Batchelor, GK. Introduction to Fluid Dynamics. Cambridge Univ. Press; Cambridge, U. K.: 1970. p. 615

Bottinga Y, Weill DF. The viscosity of magmatic silicate liquids: A model for calculation. Am J Sci. 1972; 272:438–475.

Calvari S, Coltelli M, Neri M, Pompilio M, Scribano V. The 1991–93 Etna eruption: Chronology and lava flow-field evolution. Acta Vulcanol. 1994; 4:1–4.

Cashman KV, Thornber C, Kauahikaua JP. Cooling and crystallization of lava in open channels, and the transition of pahoehoe lava to 'a'a. Bull Volcanol. 1999; 61(5):306–323.10.1007/s004450050299

Chester, DK.; Duncan, AM.; Guest, JE.; Kilburn, CRJ. Mount Etna: The Anatomy of a Volcano. Chapman and Hall; London: 1985. p. 187-228.

Costa A. Viscosity of high crystal content melts: Dependence on solid fraction. Geophys Res Lett. 2005; 32:L22308.10.1029/2005GL024303

Crisp J, Cashman KV, Bonini JA, Hougen SB, Pieri DC. Crystallization history of the 1984 Mauna Loa lava flow. J Geophys Res. 1994; 99(B4):7177–7198.10.1029/93JB02973

Cristofolini R, Menzies MA, Beccaluva L, Tindle A. Petrological notes on the 1983 lavas at Mount Etna, Sicily, with reference to their REE and Sr-Nd isotope composition. Bull Volcanol. 1987; 49(4):599–607.10.1007/BF01079965

Dobran F. Nonequilibrium flow in volcanic conduits and application to the eruptions of Mt. St. Helens on May 18, 1980, and Vesuvius in AD 79. J Volcanol Geotherm Res. 1992; 49:285–311.10.1016/0377-0273(92)90019-A

Downes MJ. Some experimental studies on the 1971 lavas from Etna. Philos Trans R Soc London, Ser B. 1973; 274:55–62.10.1098/rsta.1973.0025

Dragoni M. A dynamical model of lava flows cooling by radiation. Bull Volcanol. 1989; 51(2):88–95.10.1007/BF01081978

Einstein A. Eine neue bestimmung der molekuldimensionen. Ann Phys. 1906; 19:289–306.

Gauthier F. Field and laboratory studies of the rheology of Mount Etna lava. Philos Trans R Soc London, Ser B. 1973; 274:83–98.10.1098/rsta.1973.0028

Gay E, Nelson P, Armstrong W. Flow properties of suspensions with high solids concentration. AIChE J. 1969; 15:815–822.10.1002/aic.690150606

Getson JM, Whittington AG. Liquid and magma viscosity in the anorthite-forsterite-diopside-quartz system and implications for the viscosity-temperature paths of cooling magmas. J Geophys Res. 2007; 112:B10203.10.1029/2006JB004812

Ghiorso MS, Sachs RO. Chemical mass transfer in magmatic processes, IV. A revised and internally consistent thermodynamic model for the interpolation and extrapolation of liquid-solid equilibira in magmatic systems at elevated temperature and pressure. Contrib Mineral Petrol. 1995; 119:197–212.10.1007/BF00307281

Giordano D, Dingwell DB. Viscosity of hydrous Etna basalt: Implications for Plinian-style basaltic eruptions. Bull Volcanol. 2003; 65(1):8–14.10.1007/s00445-002-0233-2

Gregg TKP, Keszthelyi LP. The emplacement of pahoehoe toes: Field observations and comparison to laboratory simulations. Bull Volcanol. 2004; 66(5):381–391.10.1007/s00445-003-0319-5

Harris AJL, Rowland SK. FLOWGO: A kinematic thermo-rheological model for lava flowing in a channel. Bull Volcanol. 2001; 63(1):20–24.10.1007/s004450000120

Herd RA, Pinkerton H. Bubble coalescence in basaltic lava: Its impact on the evolution of bubble populations. J Volcanol Geotherm Res. 1997; 75:137–157.10.1016/S0377-0273(96)00039-X

Hess KU, Dingwell DB. Viscosities of hydrous leucogranitic melts: A non-Arrhenian model. Am Mineral. 1996; 81:1297–1300.

Ishihara, K.; Iguchi, M.; Kamo, K. Numerical simulation of lava flows on some volcanoes in Japan. In: Fink, JH., editor. Lava Flows and Domes. Springer; Berlin: 1990. p. 174-207.

Keszthelyi L, Self S. Some physical requirements for the emplacement of long basaltic lava flows. J Geophys Res. 1998; 103(B11):27,447–27,464.10.1029/98JB00606

Lipman, PW.; Banks, NG. Aa flow dynamics, Mauna Loa 1984, in *Volcanism in Hawaii*. In: Decker, RW.; Wright, TL.; Stauffer, PH., editors. U S Geol Surv Prof Pap. Vol. 1350. 1987. p. 1527-1567.

Lipman PW, Banks NG, Rhodes JM. Degassing-induced crystallization of basaltic magma and effects on lava rheology. Nature. 1985; 317:604–607.10.1038/317604a0

Llewellin EW, Manga M. Bubble suspension rheology and implications for conduit flow. J Volcanol Geotherm Res. 2005; 143:205–217.10.1016/j.jvolgeores.2004.09.018

Manga M, Loewenberg M. Viscosity of magmas containing highly deformable bubbles. J Volcanol Geotherm Res. 2001; 105:19–24.10.1016/S0377-0273(00)00239-0

Manga M, Castro J, Cashman KV, Loewenberg M. Rheology of bubble-bearing magmas. J Volcanol Geotherm Res. 1998; 87:15–28.10.1016/S0377-0273(98)00091-2

Marsh BD. On the crystallinity, probability of occurrence, and rheology of lava and magma. Contrib Mineral Petrol. 1981; 78:85–98.10.1007/BF00371146

Metrich N, Clocchiatti R. Melt inclusion behaviour in historic alkali basaltic magmas of Etna. Bull Volcanol. 1989; 51(3):185–198.10.1007/BF01067955

Metrich N, Clocchiatti R, Mosbah M, Chaussidon M. The 1989–1990 activity of Etna magma mingling and ascent of H_2O-Cl-S-rich basaltic magma. Evidence from melt inclusions. J Volcanol Geotherm Res. 1993; 59:131–144.10.1016/0377-0273(93)90082-3

Métrich N, Allarad P, Spilliaert N, Andronico D, Burton M. 2001 flank eruption of the alkali- and volatile-rich primitive basalt responsible for Mount Etna's evolution in the last three decades. Earth Planet Sci Lett. 2004; 228:1–17.10.1016/j.epsl.2004.09.036

Moore, HJ. Preliminary estimates of the rheological properties of 1984 Mauna Loa Lava, in *Volcanism in Hawaii*. In: Decker, RW.; Wright, TL.; Stauffer, PH., editors. U S Geol Surv Prof Pap. Vol. 1350. 1987. p. 1569-1588.

Pal R. Rheological behavior of bubble-bearing magmas. Earth Planet Sci Lett. 2003; 207:165–179.10.1016/S0012-821X(02)01104-4

Papale P, Dobran F. Magma flow along the volcanic conduit during the Plinian and pyroclastic flow phases of the May 18, 1980, Mount St. Helens eruption. J Geophys Res. 1994; 99(B3):4355–4373.10.1029/93JB02972

Phan-Thien N, Pham DC. Differential multiphase models for polydispersed suspensions and particulate solids. J Non Newt Fluid Mech. 1997; 72:305–318.10.1016/S0377-0257(97)90002-1

Pinkerton H, Norton G. Rheological properties of basaltic lavas at sub-liquidus temperatures: Laboratory and field measurements on lavas from Mount Etna. J Volcanol Geotherm Res. 1995; 68:307–323.10.1016/0377-0273(95)00018-7

Pinkerton H, Sparks RSJ. The 1975 sub-terminal lavas, Mount Etna: A case history of the formation of a compound lava field. J Volcanol Geotherm Res. 1976; 1:167–182.10.1016/0377-0273(76)90005-6

Pinkerton H, Sparks RSJ. Field measurements of the rheology of *lava*. Nature. 1978; 276:383–385.10.1038/276383a0

Pinkerton H, Stevenson RJ. Methods of determining the rheological properties of magmas at sub-liquidus temperatures. J Volcanol Geotherm Res. 1992; 53:47–66.10.1016/0377-0273(92)90073-M

Pompilio M, Trigila R, Zanon V. Melting experiments on Mt. Etna lavas: I–The calibration of an empirical geothermometer to estimate the eruptive temperature. Acta Vulcanol. 1998; 10(1):67–75.

Rhodes JM. Geochemistry of the 1984 Mauna Loa eruption: Implications for magma storage and supply. J Geophys Res. 1988; 93(B5):4453–4466.10.1029/JB093iB05p04453

Roscoe R. The viscosity of suspensions of rigid spheres. Br J Appl Phys. 1952; 3:267–269.10.1088/0508-3443/3/8/306

Russell JK. Crystallization and vesiculation of the 1984 eruption of Mauna Loa. J Geophys Res. 1987; 92(B13):13,731–13,743.10.1029/JB092iB13p13731

Rust AC, Manga M. Effects of bubble deformation on the viscosity of dilute suspensions. J Non Newt Fluid Mech. 2002; 104:53–63.10.1016/S0377-0257(02)00013-7

Ryerson FJ, Weed HC, Piwinskii AJ. Rheology of sub-liquidus magmas 1. Picritic compositions. J Geophys Res. 1988; 93(B4):3421–3436.10.1029/JB093iB04p03421

Sato H. Viscosity measurement of subliquidus magmas: 1707 basalt of Fuji volcano. J Mineral Petrol Sci. 2005; 100:133–142.10.2465/jmps.100.133

Shaw HR. Rheology of basalt in the melting range. J Petrol. 1969; 10(3):510–535.

Shaw HR. Viscosities of magmatic silicate liquids: An empirical method of prediction. Am J Sci. 1972; 272:870–893.

Spilliaert N, Allard P, Métrich N, Sobolev AV. Melt inclusion record of the conditions of ascent, degassing, and extrusion of volatile-rich alkali basalt during the powerful 2002 flank eruption of Mount Etna (Italy). J Geophys Res. 2006; 111:B04203.10.1029/2005JB003934

Tanguy JC. The 1971 Etna eruption: Petrology of the lavas. Philos Trans R Soc London, Ser B. 1973; 274:45–53.10.1098/rsta.1973.0024

Tanguy JC. Les éruptions historiques de l'Etna: Chronologie et localization. Bull Volcanol. 1981; 44(3):585–640.10.1007/BF02600588

Tanguy JC, Clocchiatti R. The Etnean lavas, 1977–1983: Petrology and mineralogy. Bull Volcanol. 1984; 47(4):879–894.10.1007/BF01952349

Taylor GI. The viscosity of a fluid containing small drops of another fluid. Proc R Soc London. 1932; 138:41–48.10.1098/rspa.1932.0169

Tonarini S, Armienti P, D'Orazio M, Innocenti F, Pompilio M, Petrini R. Geochemical and isotopic monitoring of Mt Etna 1989–1993 eruptive activity: Bearing on the shallow feeding system. J Volcanol Geotherm Res. 1995; 64:95–115.10.1016/0377-0273(94)00039-J

Walker GPL. Thickness and viscosity of Etnean lavas. Nature. 1967; 213:484–485.10.1038/213484a0

Whittington A, Richet P, Holtz F. Water and the viscosity of deploymerized aluminosilicate melts. Geochim Cosmochim Acta. 2000; 64(21):3725–3736.10.1016/S0016-7037(00)00448-8

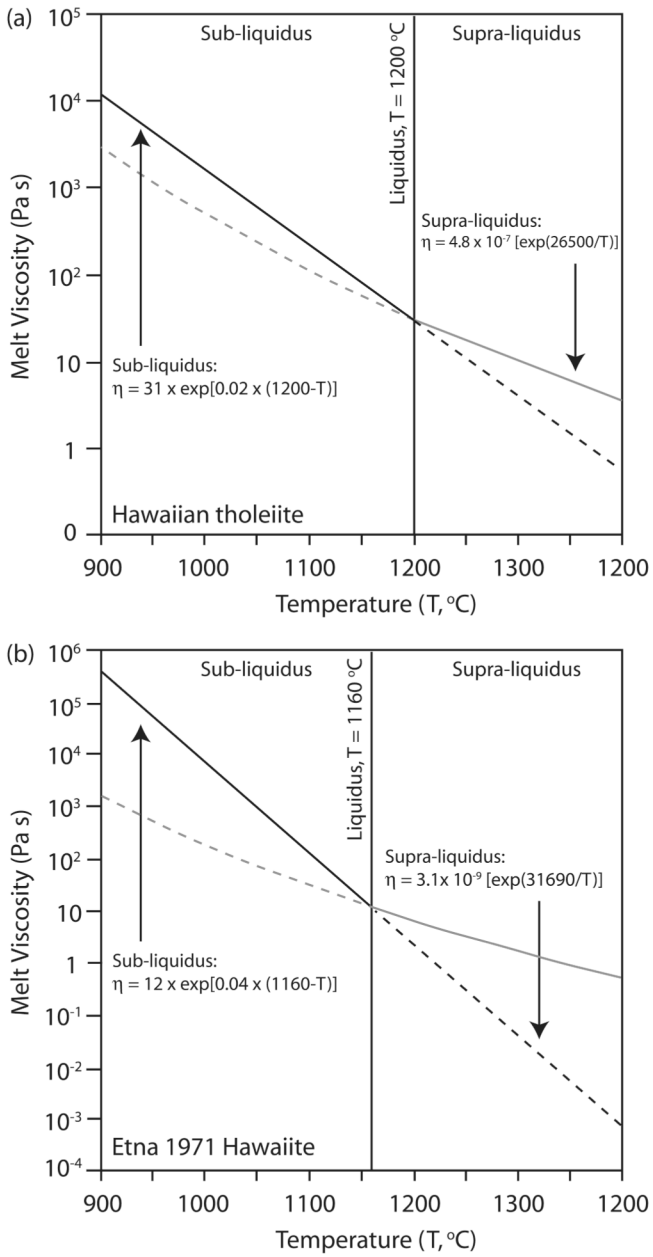

Figure 1.

Supraliquidus and subliquidus relationship between temperature and fluid viscosity defined for (a) Hawaiian tholeiite by *Shaw* [1969] and (b) Etna 1971 (Hawaiite) lavas by *Gauthier* [1973] and *Dragoni* [1989]. The supraliquidus and subliquidus relationships are given in gray and black, respectively, and are projected through the solidus (and into inappropriate temperature domains) as dashed lines. The appropriate relationships either side of the liquidus (which is given by the vertical black line) are plotted as solid lines; that is, the supraliquidus relationship is appropriate to the right of the solidus line, and the subliquidus relationship is appropriate to the left. Where each relationship becomes inappropriate, the line is dashed. This shows the error that would occur if the supraliquidus relationship was applied at subliquidus temperatures, or if the subliquidus relationship was applied at

supraliquidus temperatures. In both cases, an underestimate of the true fluid viscosity occurs.

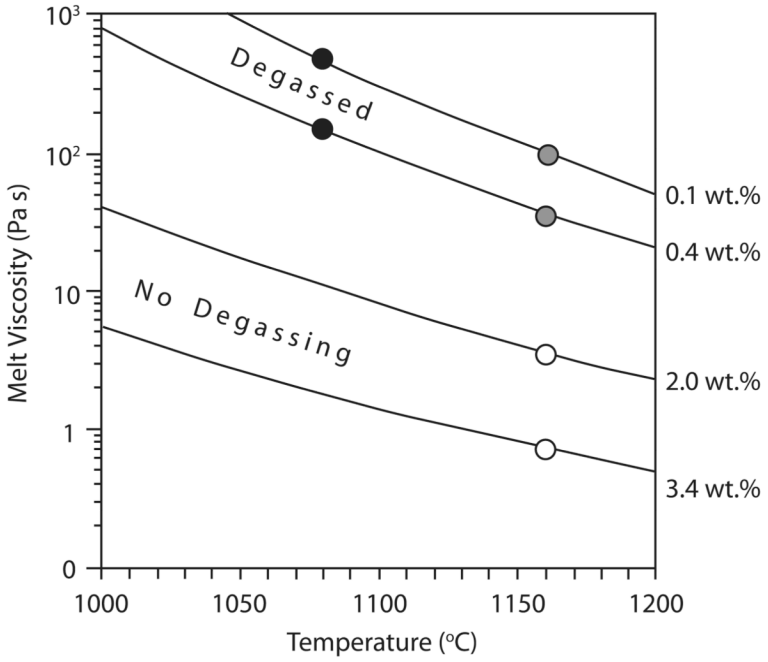

Figure 2.

Fluid viscosity for Etna alkali basalt as a function of temperature and water content following *Giordano and Dingwell* [2003] (equation (5)). Relationships are given for melt before ascent and degassing (3.4 and 2.0 wt % H_2O) and upon eruption (following water degassing with 0.1 and 0.4 wt % H_2O.) Viscosities for undegassed and degassed melt at Etna's liquidus temperature (1160°C) are located by white and gray circles, respectively; black circles locate viscosities for degassed melt at an eruption temperature of 1080°C.

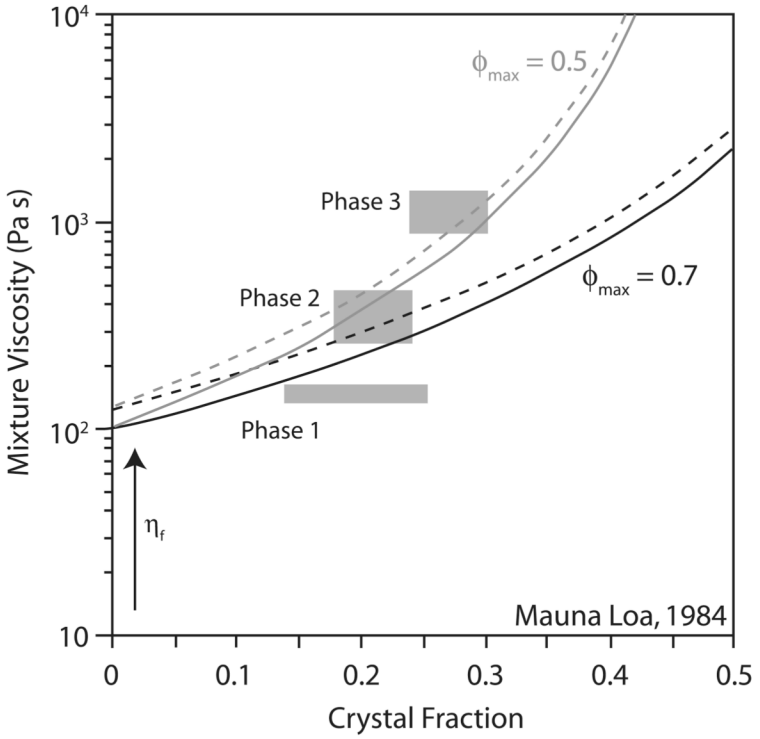

Figure 3.

Relationship between crystal content of a two-phase fluid-crystal mixture and the viscosity of that mixture estimated using the Einstein-Roscoe (equation (6)). Relationship is given for maximum particle (φ_{max}) concentrations of 70% (black line) and 50% (gray line). For each case, the relationship is plotted for a fluid phase with a viscosity (η_f) of 100 Pa s (solid lines) and 125 Pa s (dashed lines), consistent with the η_f expected for the opening and closing phases of the 1984 Mauna Loa eruption. This defines the offset on the viscosity axis. Gray zones mark the crystal contents and viscosities for the three phases of the Mauna Loa 1984 eruption defined, on the basis of viscosity, in Table 1. The formulation proposed by *Pinkerton and Stevenson* [1992] for high strain rates (equation (7)) produces, essentially, the same result.

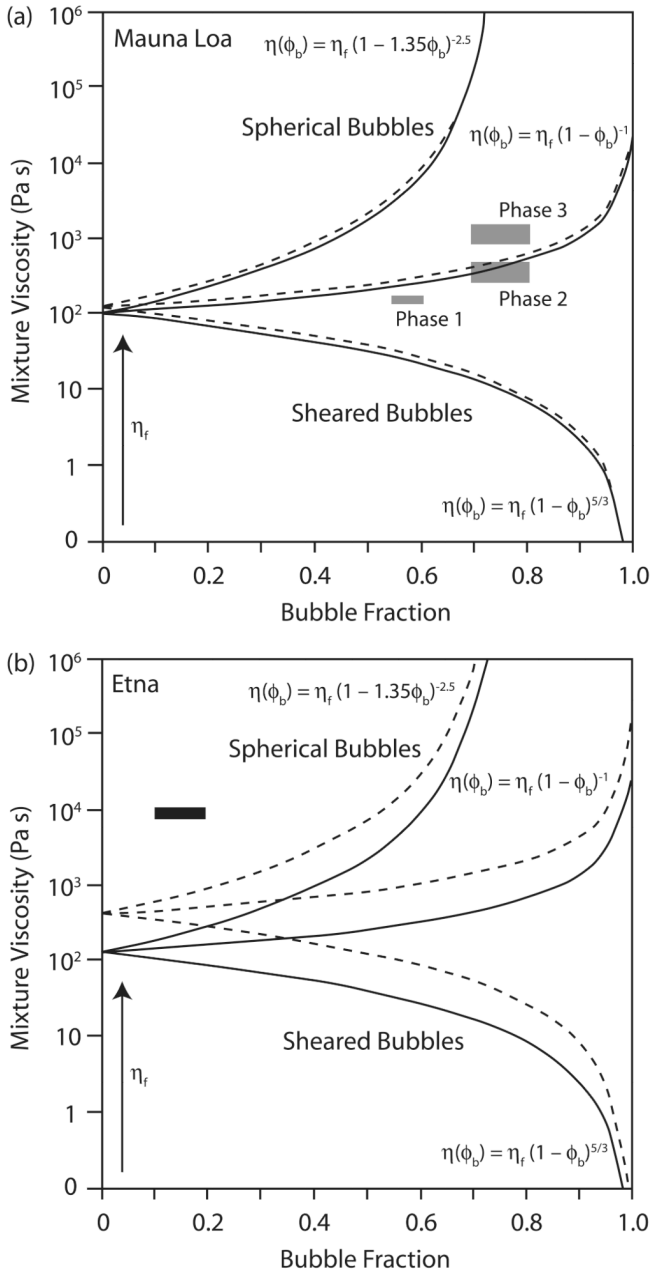

Figure 4.

Relationship between bubble content of a two phase fluid-bubble mixture and the viscosity of that mixture estimated using equations (8), (10a) and (10b), the latter being appropriate for sheared bubbles. Relationship is given for (a) Mauna Loa and (b) Etna, where the relationship is plotted for the low (solid lines) and high (dashed lines) viscosity fluid phases calculated for the two systems. This defines the offset on the viscosity axis (i.e., this gives η_f at $\varphi_b = 0$). Gray zones in Figure 4a mark the bubble contents and viscosities for the three phases of the Mauna Loa 1984 eruption defined, on the basis of viscosity, in Table 1. Horizontal bar in Figure 4b indicates the viscosity and bubble content measured by *Pinkerton* and *Sparks* [1976] giving a mixture viscosity of 9400 ± 1500 Pa s at a bubble content of 10–20%.

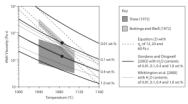

Figure 5.

Subliquidus variation in melt viscosity with temperature predicted for Etna on the basis of five different approaches. Approach 1 (dark gray zone) is the viscosity field defined by applying the work by *Shaw* [1972]. The limits are defined using the maximum (from the 1991–1993 glass composition of Table 4 with 0.01 wt % H_2O) and minimum (from the 1974 whole rock composition of Table 3 with 0.4 wt % H_2O) expected melt viscosities across an eruption temperature range of 1040–1110°C. Approach 2 (light gray zone) is the viscosity field defined by applying the method of *Bottinga and Weill* [1972]. These limits are defined using the maximum (from the 1983 glass composition of Table 4) and minimum (from the 1967 whole rock composition of Table 3) expected melt viscosities at liquidus. These are then used as input (as viscosity at liquidus, η_0) into the subliquidus temperature-dependent relationship of equation (3). Approach 3 (dashed lines) applies the subliquidus temperature-dependent relationship of equation (3) with viscosities at liquidus (η_0) of 12, 20, and 60 Pa s. Approaches 4 (thick solid lines) and 5 (thin solid lines) use the methods of *Giordano and Dingwell* [2003] and *Whittington et al.* [2000], respectively, with H_2O contents of 0.01, 0.1, 0.4, and 1.0 wt %. The two solid points mark the melt viscosities obtained from *Giordano and Dingwell* [2003] at 1086°C with H_2O contents of 0.1 and 0.4 wt %. They sit nicely within the fields defined by the other four approaches.

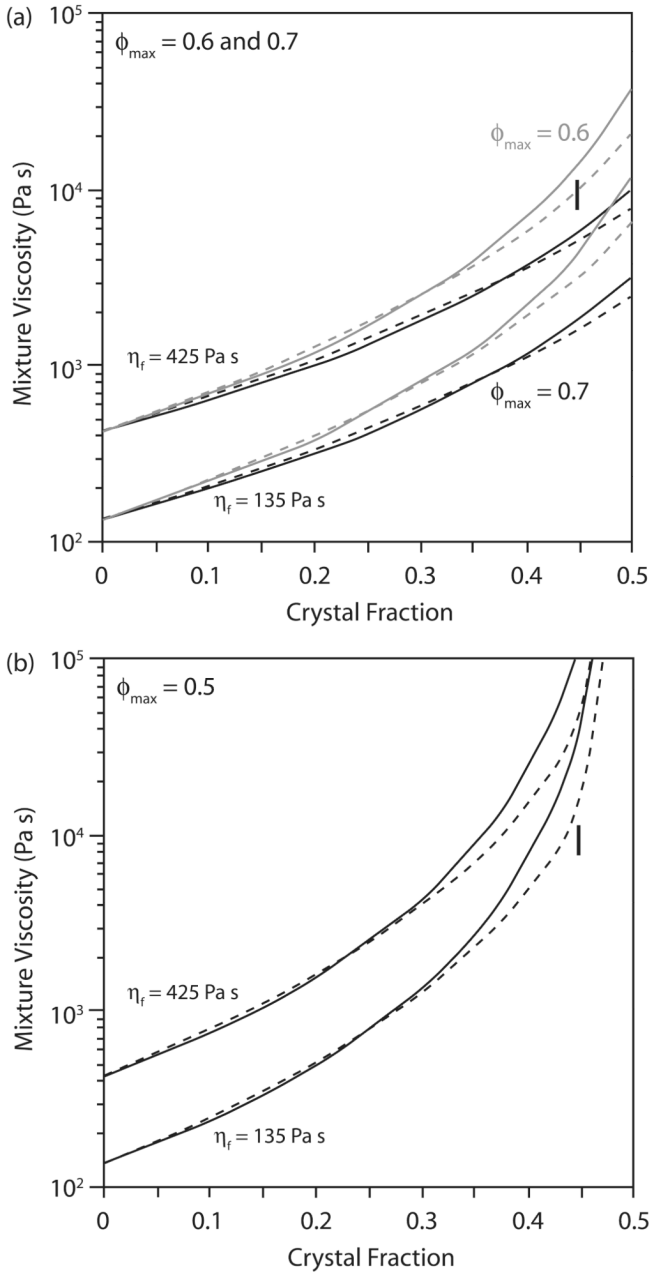

Figure 6.

Relationship between crystal content of a two-phase fluid-crystal mixture and the viscosity of that mixture estimated using Einstein-Roscoe (equation (6), solid lines) and the formulation proposed by *Pinkerton and Stevenson* [1992] for high strain rates (equation (7), dashed lines). Relationship is given for maximum particle (φ_{max}) concentrations of (a) 60% (gray lines) and 70% (black lines), as well as (b) 50%. In each case, the relationship is plotted for a fluid phase with a viscosity (η_f) of 135 and 425 Pa s, consistent with the η_f expected for undegassed (flank) and degassed (summit) lavas at Etna. This defines the offset on the viscosity axis. Vertical bar indicates the viscosity and crystal content measured by *Pinkerton and Sparks* [1976] giving a mixture viscosity of 9400 ± 1500 Pa s at a crystal content of 0.45.

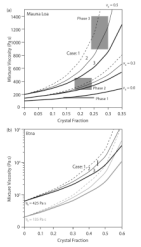

Figure 7.
(a) Variation in mixture viscosity with crystal content for a three-phase mixture with bubble volume fractions (v_b) of 0, 0.3, and 0.5 and a fluid viscosity of 100 Pa s. Gray zones mark the crystal contents and viscosities for the three phases of the Mauna Loa 1984 eruption defined, on the basis of viscosity, in Table 1. (b) Variation in mixture viscosity with crystal content for a three-phase mixture with a bubble volume fraction of 0.35 and fluid viscosities of 135 Pa s (gray lines) and 425 Pa s (black lines). Vertical bar indicates the viscosity and crystal content measured by *Pinkerton and Sparks* [1976] giving a mixture viscosity of 9400 ± 1500 Pa s at a crystal content of 0.45. In Figures 7a and 7b, three cases are plotted: (1) crystals are smaller than the bubbles (dashed lines), (2) crystals and bubbles have the same size range (thin solid lines), and (3) crystals are larger than the bubbles (thick solid lines).

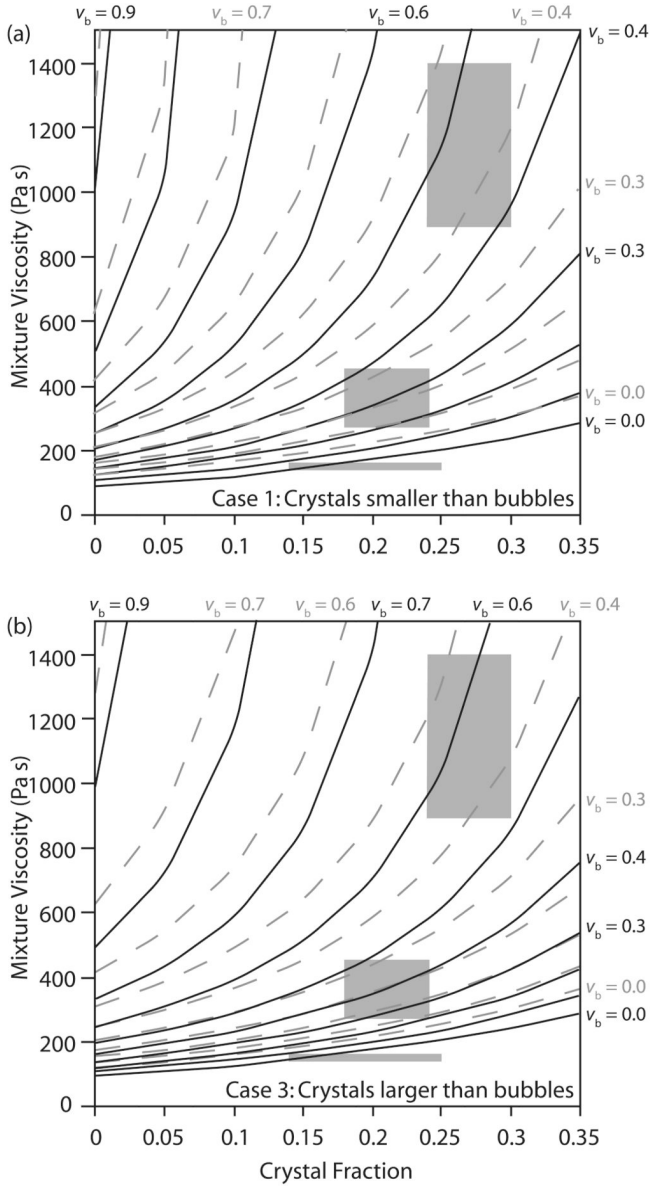

Figure 8.

Three-phase viscosity treatment for a case where (a) crystals are smaller than the bubbles (case 1) and (b) crystals are larger than the bubbles (case 3). In each case we use a fluid viscosity for Mauna Loa of 100 Pa s (black solid lines) and 125 Pa s (Figure 8b) (gray, dashed lines) and a range of bubble volume fractions (v_b) from 0 to 0.9. Gray zones mark the crystal contents and viscosities for the three phases of the Mauna Loa 1984 eruption defined, on the basis of viscosity, in Table 1.

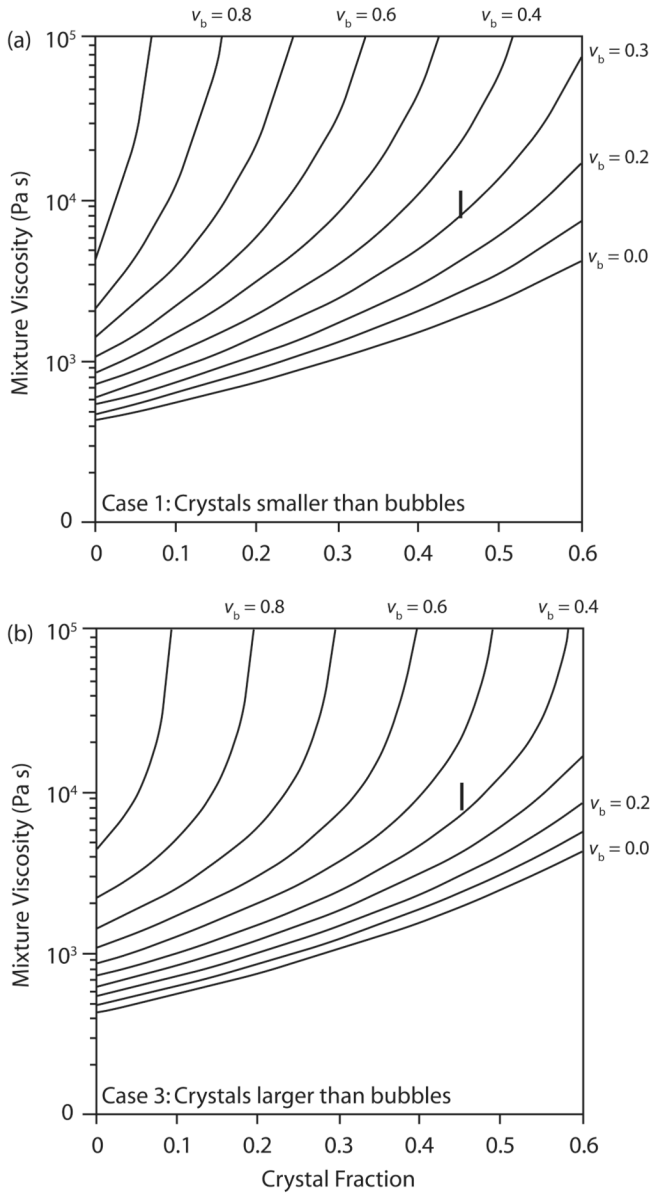

Figure 9.

Three-phase viscosity treatment for a case where (a) crystals are smaller than the bubbles (case 1), and (b) crystals are larger than the bubbles (case 3). For both cases, we use the fluid viscosity for a summit eruption of degassed lava at Etna (i.e., 425 Pa s) and a range of bubble volume fractions (v_b) from 0 to 0.9. Vertical bar indicates the viscosity and crystal content measured by *Pinkerton and Sparks* [1976].

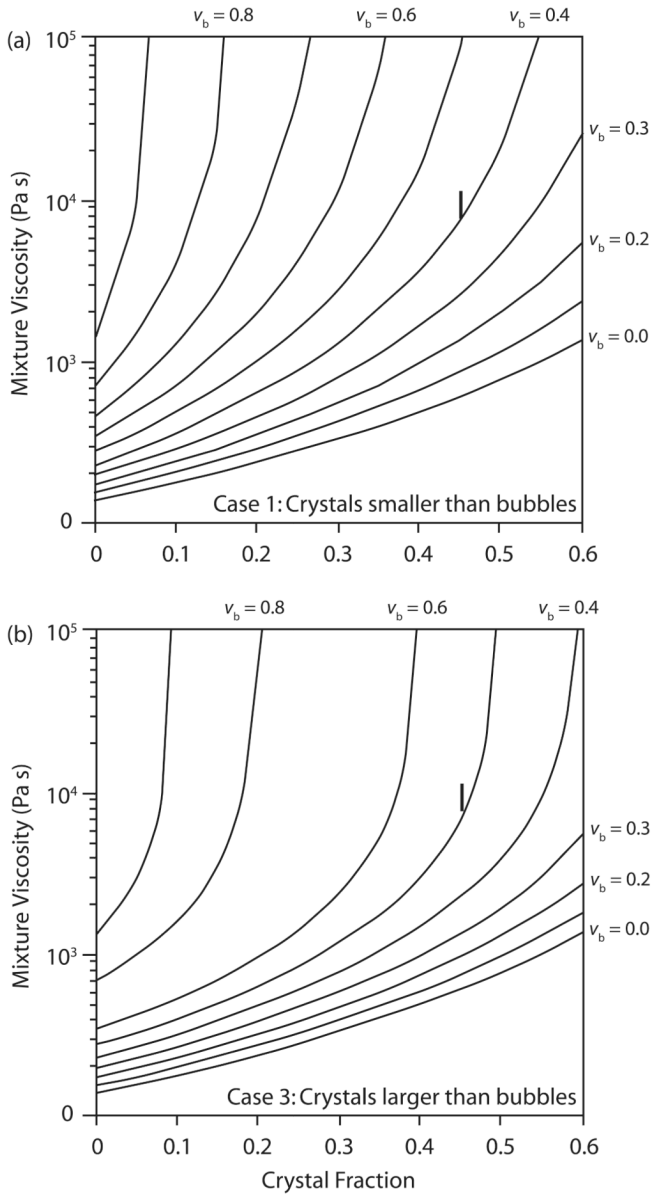

Figure 10.

Three-phase viscosity treatment for a case where (a) crystals are smaller than the bubbles (case 1) and (b) crystals are larger than the bubbles (case 2). For both cases we use the fluid viscosity for a flank eruption of poorly degassed lava at Etna (i.e., 135 Pa s) and a range of bubble volume fractions (v_b) from 0 to 0.9. Vertical bar indicates the viscosity and crystal content measured by *Pinkerton and Sparks* [1976].

Table 1

Viscosity-Crystallinity Phases for the Mauna Loa 1984 Eruption[a]

				Calculated Viscosity of Fluid-Crystal Mixture (Pa s)			
				φ_{max} = 70%		φ_{max} = 50%	
Date	**Viscosity Phase**	**Field-Derived Viscosity (Pa s)**	**Crystallinity (%)**	**η_f = 100 Pa s**	**η_f = 125 Pa s**	**η_f = 100 Pa s**	**η_f = 125 Pa s**
25 March		No data	0–7	100–133	125–170	100–150	125–190
26–28 March		No data	8–15	135–190	170–240	155–260	190–320
2–6 April	1, low	140–160	14–25	175–320	220–400	230–575	284–720
8–9 April	2, intermediate	270–450	18–24	**210–300**	**260–380**	**305–530**	**380–660**
12–13 April	3, high	900–1400	24–30	285–425	360–530	**510–930**	**640–1160**

[a]Defined using the viscosity data of *Moore* [1987] and crystal data of *Lipman and Banks* [1987]. Viscosity measurements are only available post-2 April 1984. Calculated viscosities for a fluid-crystal mixture use equations (6), minimum bound, and (7), maximum bound, with maximum crystal contents (φ_{max}) of (1) 70% (R = 1.4) and (2) 50% (R = 2.0) and fluid viscosities (η_f) of 100 and 125 Pa s. Calculated viscosities given in bold are those ranges that agree with the field-derived viscosities of *Moore* [1987].

Table 2

Whole Rock and Interstitial Glass Composition of 1984 Mauna Loa Lava Samples From *Rhodes* [1988] With Fluid Viscosities That These Give at Liquidus (T_{liquid} = 1200°C) and Eruption Temperatures (T_{erupt} = 1140°C)[a]

	Mean	ML-156 0.1[b]		ML-176 1.8[b]		ML-190 6.8[b]		ML-120 513.5[b]	
	Whole Rock	Whole Rock	Glass	Whole Rock	Glass	Whole Rock	Glass	Whole Rock	Glass
SiO_2	52.32	52.11	52.19	52.11	52.54	51.92	52.49	52.07	53.73
TiO_2	2.11	2.14	2.11	2.09	2.29	2.10	2.22	2.08	2.65
Al_2O_3	13.82	13.81	13.94	13.81	13.43	13.86	13.57	13.80	12.95
FeO (total iron expressed as FeO)	10.99	10.91	10.79	11.03	11.45	10.96	11.23	11.02	12.61
MnO	0.18	0.18	0.17	0.18	0.19	0.19	0.18	0.19	0.20
MgO	6.81	6.71	6.57	6.68	6.17	6.73	6.17	6.82	5.48
CaO	10.63	10.62	10.58	10.63	10.43	10.62	10.40	10.59	9.78
Na_2O	2.36	2.53	2.55	2.4	2.57	2.55	2.49	2.42	2.36
K_2O	0.39	0.39	0.38	0.4	0.41	0.38	0.39	0.39	0.47
P_2O_5	–	0.25	–	0.26	–	0.23	–	0.25	–
Total	99.61	99.51	99.28	99.60	99.46	99.55	99.14	99.64	100.25
Viscosity at T_{liquid} [*Bottinga and Weill*, 1972][c]	38	35	37	37	37	35	39	36	46
Viscosity at T_{liquid} [*Shaw*, 1972][d]	44	42	46	44	49	41	51	42	62
Viscosity at T_{liquid} (equation (2))	31	31	31	31	31	31	31	31	31
Viscosity at T_{erupt} (method 1, *Bottinga and Weill* [1972])[c]	126	116	123	123	123	116	129	120	153
Viscosity at T_{erupt} (method 2, *Shaw* [1972])[d]	86	83	91	86	96	81	102	83	125
Viscosity at T_{erupt} (method 3, equation (3))	103	103	103	103	103	103	103	103	103

[a]Mean whole rock composition is the average of all 67 samples analyzed by *Rhodes* [1988], as given in Table 4 of *Rhodes* [1988]. Whole rock and glass compositions for selected samples from different times during the eruption (samples ML-156 to ML-120) are taken from Table 3 of *Rhodes* [1988]. To assess fluid viscosity at liquidus, we use (1) *Bottinga and Weill* [1972], (2) *Shaw* [1972], and (3) temperature-dependent viscosity from equation (2). To assess the likely viscosity at eruption (subliquidus) temperature, we apply the following three methods. Method 1 uses viscosity at liquidus (η_0) obtained using *Bottinga and Weill* [1972] to obtain subliquidus fluid viscosity at eruption temperature using equation (3). Method 2 applies *Shaw* [1972] with T equal to eruption temperature (equation (4)). Method 3 uses the temperature-dependent (equation (2)) viscosity at liquidus (η_0) in equation (3) to gain a subliquidus temperature dependence with, for the Mauna Loa 1984 case, T_O = 1200°C and T_L = 1140°C.

[b]Time since start of eruption (hours).

[c] Calculated using Fe_2O_3 and FeO obtained from total FeO using Wt % ratio of $Fe_2O_3/(Fe_2O_3 + FeO)$ of 0.15 [*Crisp et al.*, 1994].

[d] Calculated with 0.1 wt % H_2O [*Russell*, 1987].

Table 3

Summary of Published Whole Rock Composition of Etna's 1967–1989 Lavas Emplaced During Summit and Flank Eruptions, With Water Content Where Available[a]

	Eruption								
	1967	**1971**	**1973**	**1974**	**1975**	**1978**	**1979**	**1980**	**1989**
Location[b]	summit	flank	summit	flank	summit	flank	flank	summit	flank
Source reference	1	1, 2	3	3	3	4	4	4	5
Number of analyses	1	15	2	16	2	6	3	5	19
SiO_2	47.4	47.5	48.9	47.1	48.8	47.6	47.8	48.1	47.7
TiO_2	1.7	1.7	1.6	1.6	1.7	1.7	1.7	1.7	1.8
Al_2O_3	17.1	16.7	17.6	18.2	17.7	17.2	17.3	17.7	17.8
Fe_2O_3	3.2	4.4	–	–	–	4.1	3.9	3.5	3.4
FeO	7.6	6.7	9.8	9.7	10.0	6.6	6.7	6.7	7.0
MnO	0.2	0.2	0.2	0.2	0.2	0.2	0.2	0.2	0.2
MgO	5.5	5.2	5.4	6.8	4.8	5.6	5.4	5.3	5.5
CaO	10.3	11.0	10.2	10.4	10.0	10.6	10.5	10.3	10.3
Na_2O	4.0	3.8	3.9	3.7	4.3	3.9	3.9	4.0	3.5
K_2O	1.8	1.7	1.8	1.9	1.9	1.9	1.9	1.9	1.9
P_2O_5	0.4	0.5	0.6	0.4	0.6	0.5	0.5	0.6	0.4
H_2O	0.1	0.4	–	–	–	–	–	–	–
Total	99.1	99.8	100	100	100	100	100	100	99.5
Viscosity at T_{liquid} [*Bottinga and Weill*, 1972]	16	17	27	22	26	17	17	19	21
Viscosity at T_{liquid} [*Shaw*, 1972][c]	34	27	53	20	57	25	26	40	30
Viscosity at T_{liquid} (equation (2))	12	12	12	12	12	12	12	12	12
Viscosity at T_{erupt} (method 1, *Bottinga and Weill* [1972])	389	419	662	540	638	419	419	466	515
Viscosity at T_{erupt} (method 2, *Shaw* [1972])[c]	86	66	137	47	149	63	63	103	73
Viscosity at T_{erupt} (method 3, equation (3))	305	305	305	305	305	305	305	305	305

[a]Averages are given from the referenced sources. Fluid viscosities for each average composition are given at liquidus (T_{liquid} = 1160°C) and eruption temperatures (T_{erupt} = 1080°C). To assess fluid viscosity at liquidus and upon eruption (subliquidus) temperature, we apply the same methods as followed in Table 2, with the input parameters set appropriate to Etna. Source references: 1, *Tanguy* [1973]; 2, *Downes* [1973]; 3, *Armienti et al.* [1984]; 4, *Tanguy and Clocchiatti* [1984]; and 5, *Tonarini et al.* [1995].

[b] For exact eruption location and details, see *Tanguy* [1981].

[c] For cases where H_2O is not available, H_2O of 0.1 wt % is used for summit eruptions and 0.4 wt % is used for flank eruptions.

Table 4

Published Whole Rock and Glass Compositions for Lavas Emplaced During Etna's 1983 and 1991–93 Flank Eruptions[a]

	Eruption			
	1983		1991–93	
	Whole Rock	Glass	Whole Rock	Glass
Source reference	1	2	3	4
Number of analyses	18	3	20	2
SiO_2	46.8	50.4	47.9	51.8
TiO_2	1.8	1.9	1.7	2.0
Al_2O_3	17.7	16.8	17.9	16.0
Fe_2O_3	3.6	–	3.3	4.6
FeO	6.8	10.4	7.0	6.5
MnO	0.2	0.2	0.2	0.2
MgO	5.7	3.2	5.4	3.0
CaO	10.7	7.6	10.0	6.9
Na_2O	3.7	5.1	3.8	5.7
K_2O	1.8	3.5	1.9	3.4
P_2O_5	0.5	–	0.4	–
Total	99.3	99.2	99.5	100.0
Viscosity at T_{liquid} [*Bottinga and Weill*, 1972]	17	27	20	19
Viscosity at T_{liquid} [*Shaw*, 1972][b]	23	75	32	81
Viscosity at T_{liquid} (equation (2))	12	12	12	12
Viscosity at T_{erupt} (method 1, *Bottinga and Weill* [1972])	417	662	491	466
Viscosity at T_{erupt} (method 2, *Shaw* [1972])[b]	75	201	81	218
Viscosity at T_{erupt} (method 3, equation (3))	305	305	305	305

[a] Averages are given from the referenced sources. Fluid viscosities for each average composition are given at liquidus (T_{liquid} = 1160°C) and eruption temperatures (T_{erupt} = 1080°C). To assess the fluid viscosity at liquidus and upon eruption (subliquidus) temperature, we apply the same methods as followed in Table 2, with the input parameters set appropriate to Etna. Source references: 1, *Armienti et al.* [1984]; 2, *Cristofolini et al* [1987]; 3, *Tonarini et al.* [1995]; and 4, *Armienti et al.* [1994a].

[b] Calculated using 0.4 wt % H_2O.